Molecular Crystals and Liquid Crystals
Publication details, including instructions for authors and subscription information:
http://www.tandfonline.com/loi/gmcl16

Biaxial Optical Properties of Thermotropic Random Copolyesters

C. Viney [a] , G. R. Mitchell [a] & A. H. Windle [a]
[a] Department of Metallurgy, Materials Science, University of Cambridge, Cambridge, U.K.
Version of record first published: 07 Mar 2011.

To cite this article: C. Viney , G. R. Mitchell & A. H. Windle (1985): Biaxial Optical Properties of Thermotropic Random Copolyesters, Molecular Crystals and Liquid Crystals, 129:1-3, 75-108

To link to this article: http://dx.doi.org/10.1080/15421408408084167

Mol. Cryst. Liq. Cryst., 1985, Vol. 129, pp. 75–108
0026-8941/85/1293–0075/$30.00/0

Biaxial Optical Properties of Thermotropic Random Copolyesters†

C. VINEY, G. R. MITCHELL‡ and A. H. WINDLE

Department of Metallurgy and Materials Science, University of Cambridge, Pembroke Street, Cambridge CB2 3QZ, U.K.

(*Received August 16, 1984*)

The optical microstructures of thin sections of two liquid crystalline polymers are examined in the polarizing microscope. The polymers are random copolyesters based on hydroxybenzoic and hydroxynaphthoic acids (B-N), and hydroxybenzoic acid and ethylene terephthalate (B-ET). Sections cut from oriented samples, so as to include the extrusion direction, show microstructures in which there is no apparent preferred orientation of the axes describing the local optical anisotropy. The absence of preferred orientation in the microstructure, despite marked axial alignment of molecular chain segments as demonstrated by X-Ray diffraction, is interpreted in terms of the polymer having biaxial optical properties. The implication of optical biaxiality is that, although the mesophases are nematic, the orientation of the molecules is correlated about three (orthogonal) axes over distances greater than a micron. The structure is classified as a **multiaxial nematic**.

INTRODUCTION

A considerable number of polymers has been observed to exhibit thermotropic liquid crystalline behaviour;[1–4] however, the long chain nature of the molecules poses special problems in their characterization as liquid crystals. Polymer molecules offer the possibility of chemical heterogeneity as well as a significant distribution of molar mass; there are also many possible morphologies arising from the different ways in which such molecules can pack to fill space. Poly-

†Paper presented at the 10th International Liquid Crystal Conference, York, 15th–21st July 1984.

‡J. J. Thomson Laboratory, University of Reading, Whiteknights, Reading RG6 2AF.

meric systems which form liquid crystalline phases as a consequence of mesogenic units along the backbone (as opposed to in the side-groups), can be subdivided[5,6] into those in which such units are effectively decoupled from each other by highly flexible sections of polymer chain, and those in which they are closely coupled so that the molecule as a whole has little flexibility. In decoupled systems the individual mesogenic units are similar in molar mass to those in traditional (small molecule) liquid crystal-forming compounds, and the structures which they adopt are also similar, although perhaps there is a greater incidence of smectic phases.[7] Nevertheless, the accepted structural classification[8,9] appears generally appropriate to decoupled polymers. For highly coupled liquid crystalline polymers the situation is not as straightforward, since the rigid molecules may be more than 100 nm long, with a wide distribution of molar masses. Furthermore, the molecules are often randomly copolymerized as a means of reducing the crystalline-to-mesophase transition temperature into a processable range.

This paper focusses attention on the optical microstructure of rigid-chain copolyesters, and, in relating these observations to X-Ray measurements of the molecular director orientation, concludes that the polymers are nematic yet optically biaxial.

MATERIALS

Two rigid-chain thermotropic systems have formed the basis of this work. The first is a random copolymer of hydroxybenzoic and hydroxynaphthoic acids[10] in number fractions of 0.7 and 0.3 respectively, and will be referred to as B-N:

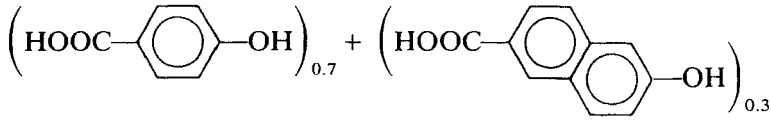

The molecule has little facility for sharp changes in trajectory and its flexibility is limited to bond distortions. Typical degrees of polymerization for this range of materials are between 100 and 200, and the softening point is in the range 280–300°C. X-Ray observations of oriented samples confirm that the copolymerization is essentially random, with no evidence of any trend towards "blockiness."[11,12]

The second system, examined in parallel, is also a random copolyester. It consists of hydroxybenzoic acid and units of the polymer

polyethylene terephthalate, in fractions of 0.6 and 0.4 respectively, and is referred to as B-ET:

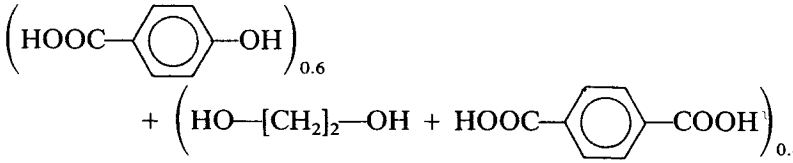

The polymer has received considerable attention as it was one of the first rigid chain thermotropic polymers to be synthesized in any quantity.[13] The presence of short flexible links, (—O—CH_2—CH_2—O—), is apparently insufficient to allow the rigid mesogenic units to decouple, although these links are probably responsible for the lower mesophase-isotropic transition temperature compared with B-N. There is also evidence from thermal analysis[14] as well as from mechanical behaviour that the polymer contains some material which does not melt until about 250°C. It is possible that this is unreacted PET present as an impurity.

OPTICAL MICROSTRUCTURE OF THIN FILMS

The optical microstructure of B-ET has already been characterised as a function of temperature.[14,15] It was found that a mesophase microstructure observed at elevated temperature could be retained by rapid cooling to room temperature, the only property to be lost being its mobility. In general, the textures observed were of the Schlieren type, although, when held between glass slides at elevated temperatures, they eventually adopted the so called "interrupted Schlieren" texture below 350°C and also developed the well documented two and four brush features associated with singularities. The most striking difference from the familiar textures shown by small molecule liquid crystals is one of scale. Even after substantial periods above the softening temperature the scale of the microstructure remains very fine, of the order of a few microns only. This aspect places considerable demands on the technique of optical microscopy, particularly at elevated temperatures.

Figure 1 shows micrographs of optical textures of the polymers B-N and B-ET observed between crossed polars. In addition to the fine scale it can be seen that the nature of the texture is unchanged on cooling from the mobile mesophase region to room temperature. In each case the microstructure can be interpreted as a variation with

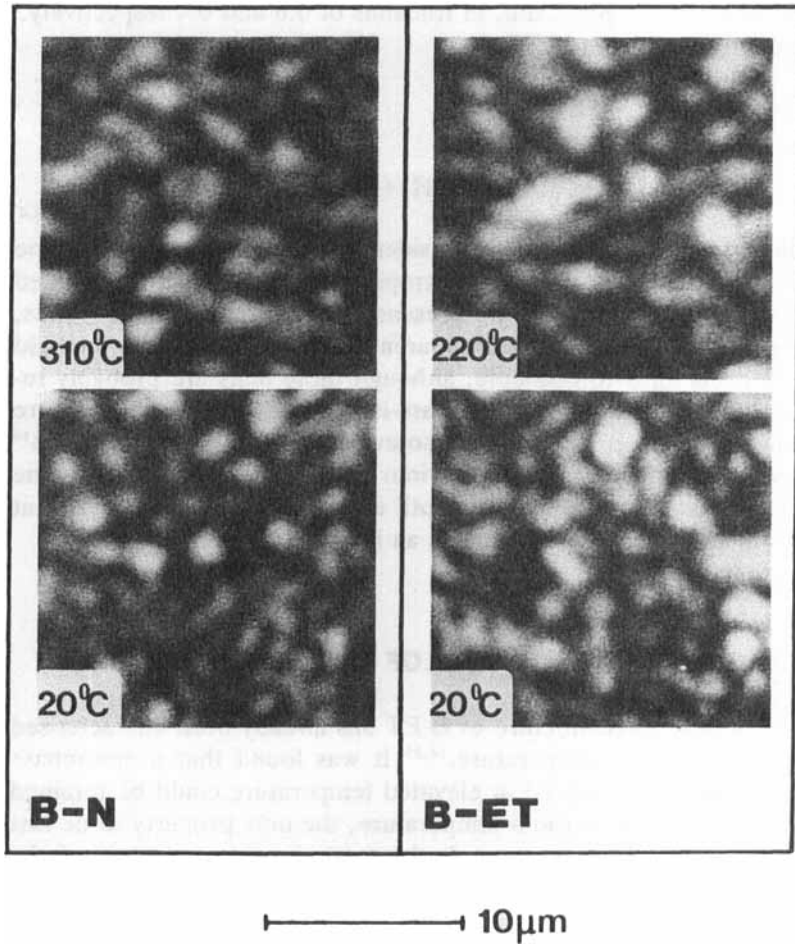

FIGURE 1 Thin sections of the polymers B-N and B-ET between crossed polars. The lower micrograph of each pair illustrates that the qualitative features of the high temperature mesophase textures are retained on cooling to room temperature. The cooling rate was of the order of 10°C. sec^{-1}.

position of the orientation of the anisotropic optical properties of the material, as defined by the orientation of the principal axes of the optical indicatrix sectioned in the plane of the sample. The thickness of the sections was about 5 μm.

MICROSTRUCTURE OF MACROSCOPICALLY ORIENTED MATERIAL

(i) *X-Ray characterization of orientation*

Rod samples, 2 mm in diameter, were supplied as extruded from the mesophase into air. They had not been subsequently drawn, but nevertheless showed substantial levels of axial alignment in the wide angle X-Ray diffraction patterns prepared with the beam normal to the extrusion axis. The ability to achieve high levels of molecular alignment from comparatively modest extensional flows is a characteristic of polymeric mesophases. Contour plots of these scattering patterns are shown for B-N and B-ET respectively in Figures 2a and 3a; the results are presented as reduced intensity functions, $si(s, \alpha)$.† Analysis of these data using the method of spherical harmonics[16] indicates that the global orientation of the lengths of chain segments which contribute coherently to the scattering is defined by values of P_2 of 0.65 for B-N[17] and 0.72 for B-ET. (P_2 is equivalent to the "order parameter," S). X-Ray diffraction was also used to confirm the axial symmetry of the sample and that there was no variation in the degree of orientation across its diameter.

Another important aspect of these diffraction patterns is that although they were prepared at room temperature, well below the softening temperature, there is no evidence of peaks sharp enough to be interpreted in terms of crystallinity. Thus, on this basis alone, it appears that the solid material has more of the attributes of a liquid crystalline glass than those of a crystalline phase. However, it should be noted that other related copolyester systems, and indeed the two examined if subjected to annealing treatments just below the softening temperature, can sometimes show sharp, albeit weak, crystal-like reflections.

(ii) *Optical microstructure*

Figures 2(b) and 3(b) show the optical textures in thin sections microtomed from the sample on a plane containing the extrusion axis.

---

†where $s = 4\pi \sin\theta/\lambda$ and α is the angle to the unique axis of the sample and:

$$i(s, \alpha) = I_{corr.}(s, \alpha) - \Sigma f^2(s)$$

where $I_{corr.}$ is the fully corrected intensity function and $f^2(s)$ the independent coherent scattering.

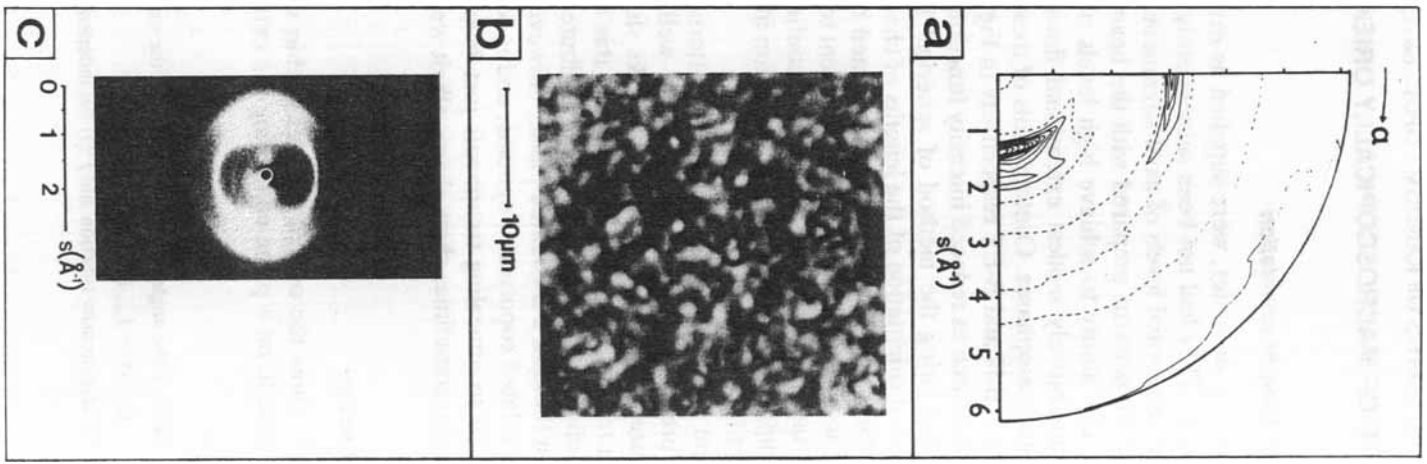

FIGURE 2 Comparison of X-Ray diffraction patterns with textures seen between crossed polars for an oriented sample of B-N. The extrusion axis is vertical in each case. (a) Contour plot of the diffracted intensity of the extruded sample expressed as reduced intensity, $si(s, \alpha)$. (b) Texture of thin section containing the extrusion axis. (c) X-Ray microbeam photograph of the same area as that shown in the micrograph.

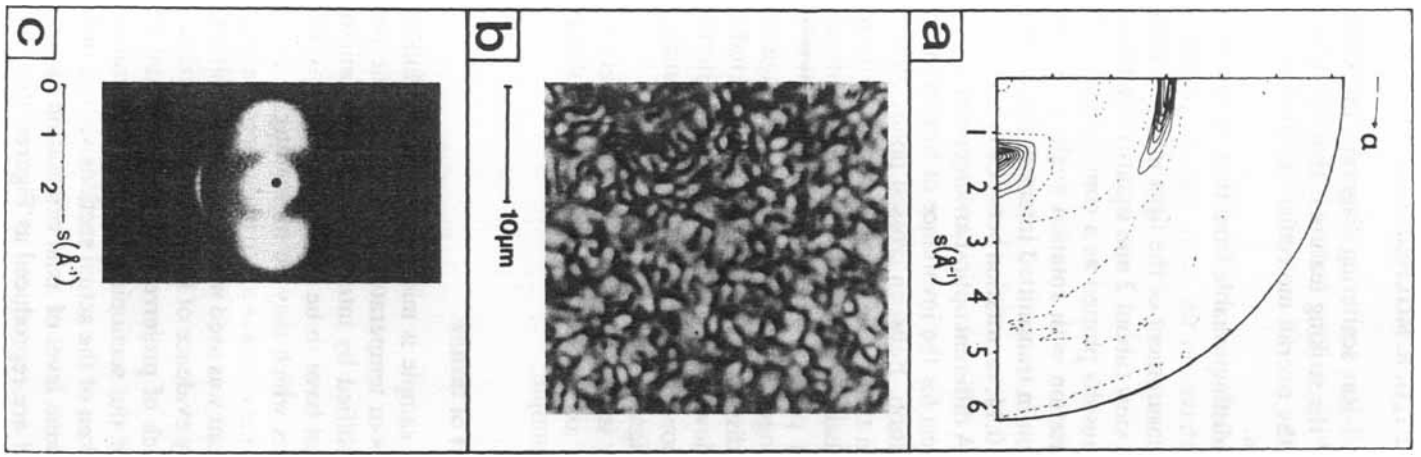

FIGURE 3 Comparisons as in Figure 2, for the polymer B-ET.

In accord with the X-Ray scattering diagrams, the axis is vertical. As noted previously,[18] the striking feature is that the optical textures do not reflect any of the overall molecular orientation apparent in the diffraction patterns.

The texture is indistinguishable from that of an unoriented sample (Figure 1), and behaves in the same way on rotation between the crossed polars. Measurement of the light intensity integrated over a substantial field of view (about 2 mm square) as a function of sample rotation gave the results plotted as a continuous line in Figure 4(a) and 4(b). The variation with rotation angle is negligible. For emphasis, the variation in transmitted intensity for a sample of PMMA oriented to a P_2 of 0.14, on rotation between crossed polars, is plotted on the same axes. A different optical arrangement was used to provide a more stringent test for the invariance of total transmitted intensity under sample rotation. Between crossed polars alone there is a 0°–90° degeneracy, in that the fast and slow vibrations in the plane of the sample are indistinguishable. However the additional introduction of a sensitive tint plate in the 45° orientation between the polars enables such orthogonal orientations to be distinguished by colour. The blue-yellow distinction obtained was converted to transmitted intensity by a yellow filter, and the results are plotted in Figure 5. Again, the variation in the total transmitted intensity as the sample is rotated is not significant.

The conclusion is clear that, as observed, there is no preferred orientation of the axes describing the local optical anisotropy within the plane of the sample.

(iii) *Interpretation of texture*

The fact that the sample is microtomed from a bulk specimen, and is examined at room temperature, means that the possibility of the texture being modified by interaction with the microscope slide or cover slip does not have to be considered. However microtomy can introduce artefacts which may be misleading if they are not recognized, and very great care was taken in the preparation of the sections. A sledge instrument was used with a feed modification,[19] and samples which showed any evidence of knife marks were discarded. As a final check that the lack of preferred orientation in the textures was not a consequence of the sectioning process, transmission X-Ray photographs were taken of the actual sections viewed in the microscope. They show the same level of axial orientation as recorded from the bulk samples and are reproduced as Figures 2(c) and 3(c).

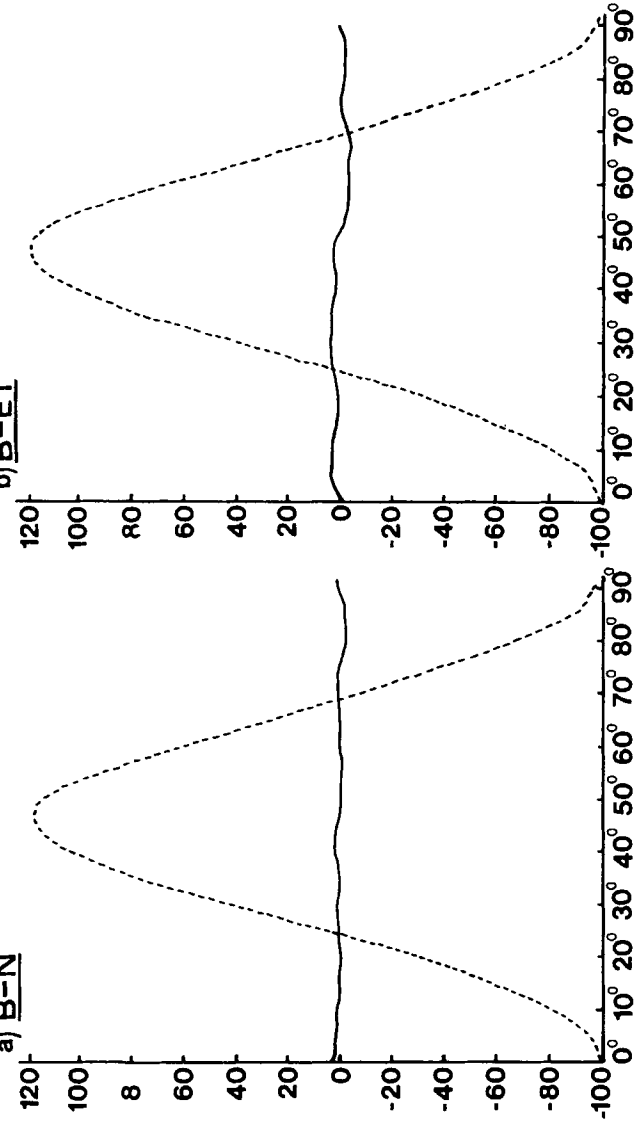

FIGURE 4 Measurements (continuous line) of light intensity transmitted through a substantial area of the thin sections (depicted in Figures 2(b) and 3(b)) as a function of the orientation of the crossed polars: (a) B-N and (b) B-ET. The intensity function F has been normalised to the transmitted intensity averaged over all crossed polar orientations. The dashed curves show equivalent plots for a sample of glassy PMMA with an orientation function $\langle P_2 \rangle$ of 0.14 measured from X-Ray diffraction data.

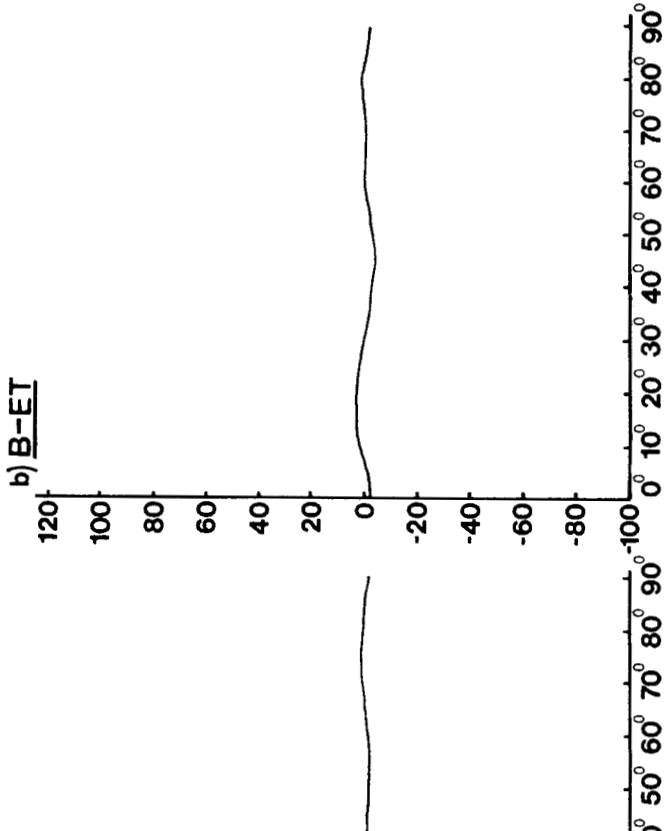

FIGURE 5 A plot of the same normalised intensity function as in Figure 4, but for yellow light and with a sensitive tint plate inserted in the 45° orientation between the crossed polars. (a) B-N. (b) B-ET.

The sections were between 4 and 6 μm thick, which is of the same order as the scale of the microstructure. A series of varying thicknesses was also examined.[20] The nature of the texture appeared independent of section thickness right down to a minimum achievable value of 2 μm, although the contrast began to decrease significantly at greater than 10 μm. The fact that superimposed sections of distinctly different optical orientations (such that guiding is not a factor) will normally show anisotropy, with the orientation of the in-plane axes lying between those of the component layers, can be demonstrated (Reference 21 and Appendix 1). It is thus not possible that the absence of preferred orientation in the 5 μm sections can be the result of through-thickness superposition of orientations.

Figures 6 and 7 show the same regions, for B-N and B-ET respectively, for different orientations of the crossed polars. It can be seen that the transmitted intensity at any point passes through a full light-dark-light type sequence, for a $\pi/2$ rotation of the polars. As a further illustration, Figures 8 and 9 are plots of the intensities measured at the bottom right-hand corners of each series of micrographs. In each case the expected $(\sin)^2$ relation is apparent. Finally, the same area was photographed without polars (Figures 6 and 7 again) and there is no microstructure apparent which could be related to that seen between crossed polars. These more detailed observations thus confirm the conclusions of the previous section:

(a) The polymer samples show local optical anisotropy.

(b) The orientation of this anisotropy (within the specimen plane) changes with position on a scale of a few microns.

(c) Despite the preferred alignment of the local molecular chain axes with the specimen extrusion axis as indicated by the diffraction patterns, there is no preferred orientation of the regions of local optical anisotropy within the plane of the specimen.

(iv) *Influence of temperature*

On heating B-N to 30°C above its softening point, the microstructure has the same appearance. It is however mobile, with areas of dark and light contrast changing position on a time scale of about one second. Figure 10 shows a sequence of micrographs taken at 310°C at 15 second intervals. The diffraction patterns, prepared from the same thin samples quenched to room temperature, show that over 45 seconds the preferred axial orientation of the chain segments is all but lost. It is thus not possible to prove for this sample that the lack of correlation between X-Ray orientation and the preferred ori-

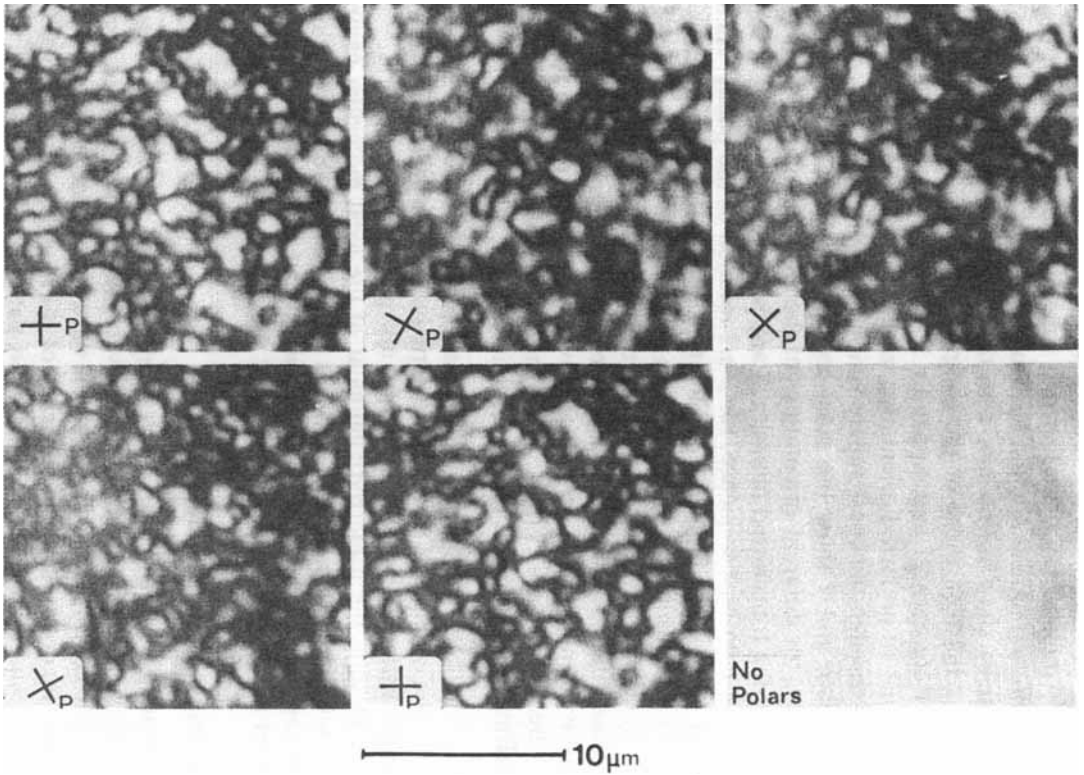

FIGURE 6 An area of the section of B-N, photographed for different orientations of the crossed polars. The final frame shows the absence of related contrast when the polars are removed.

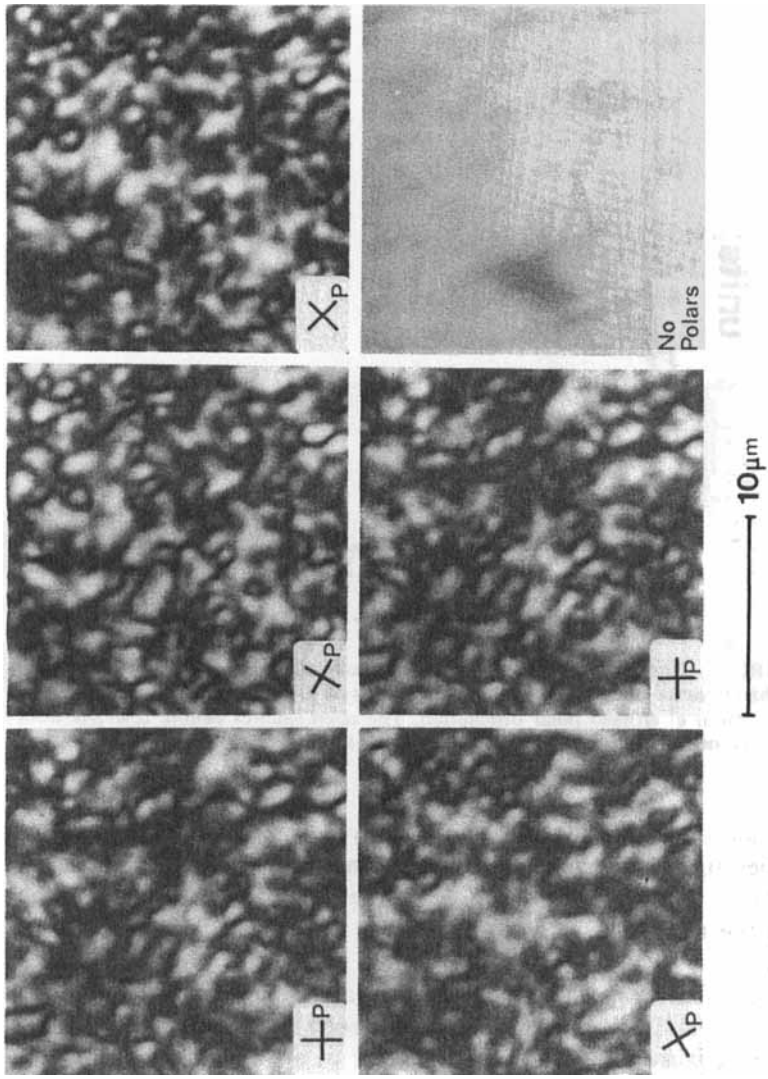

FIGURE 7 As for Figure 6, but for the polymer B-ET.

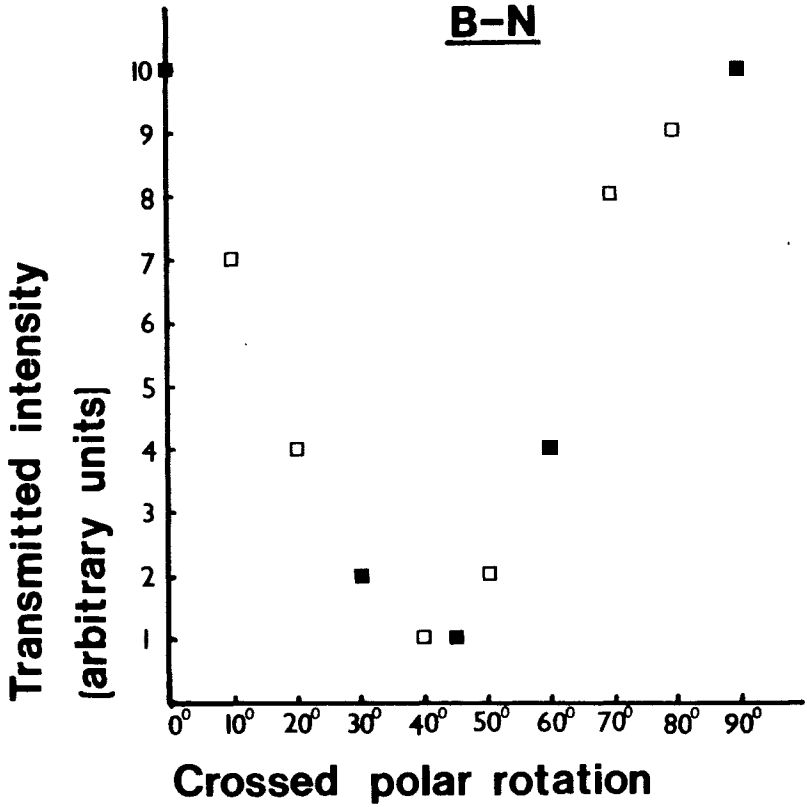

FIGURE 8 Transmitted intensity (on an arbitrary scale), measured at the bottom right-hand corner of the field of the micrographs of B-N shown in Figure 6, plotted as a function of crossed polar orientation. The open squares denote readings from additional micrographs not reproduced in Figure 6.

entation of the local optical anisotropy persist above the softening temperature. However, the generally unaltered nature of the texture and the fact that the decay of X-Ray orientation was if anything slower than the time scale of texture mobility are perhaps pointers in that direction.

The behaviour of the B-ET sample above its 'softening' temperature of 190°C is different. Firstly, between 190°C and 250°C it is not completely molten but is rather similar to a soft gel, which may be related to the presence of small regions of PET which do not melt out until the higher temperature. Within this temperature range the optical texture is mobile, just as with B-N at 310°C, but the X-Ray orientation does not decay significantly on the same time scale. Figure

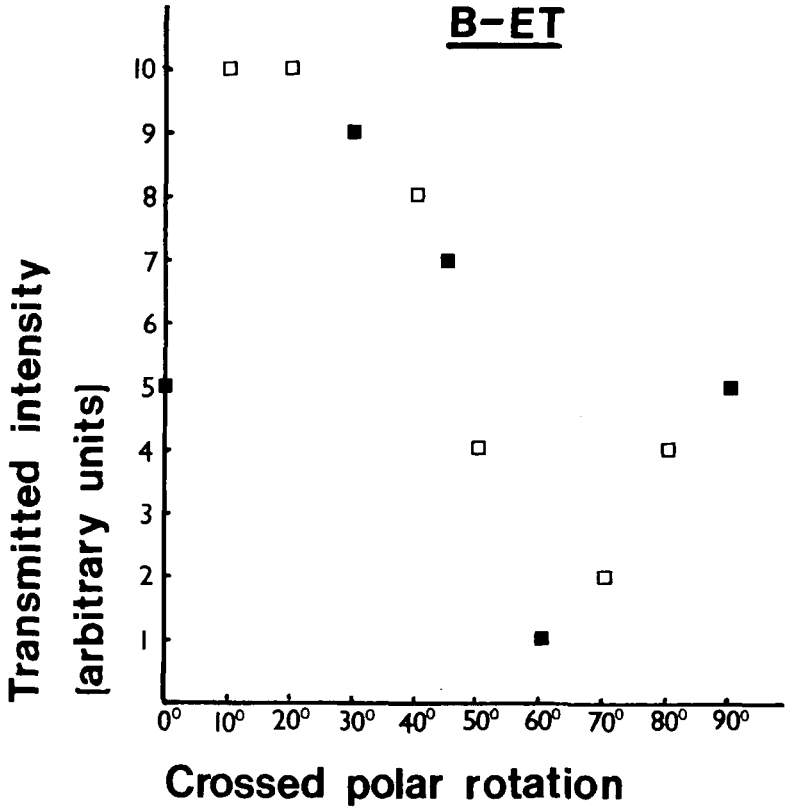

FIGURE 9 A similar plot as Figure 8, but referring to the polymer B-ET and Figure 7.

11 shows the microstructure of B-ET at 220°C. Its mobility is obvious, yet after 10 minutes the X-Ray orientation is still largely preserved. In fact periods of several hours at this temperature are necessary before the X-Ray pattern loses all its preferred orientation. So again there is evidence that the principal axes which define the local optical orientation are not directly related to the axis which is the molecular chain director within the same locality.

BIAXIAL OPTICAL PROPERTIES

The purpose of this section is to address a particular geometric question. If the optical properties of a local anisotropic region are the most general possible, that is **biaxial**, and one of the principal axes

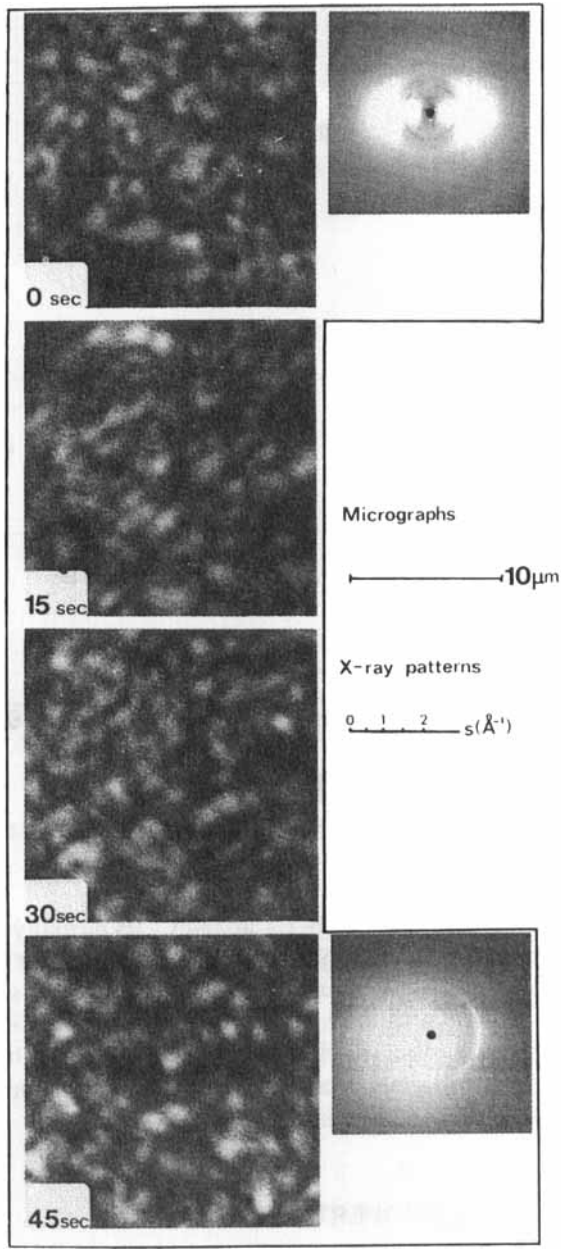

FIGURE 10 A sequence of micrographs of B-N at 310°C, taken at 15 second intervals. The texture is seen to be mobile, and most of the X-Ray orientation (determined at room temperature from the same thin sections) has decayed after 45 seconds.

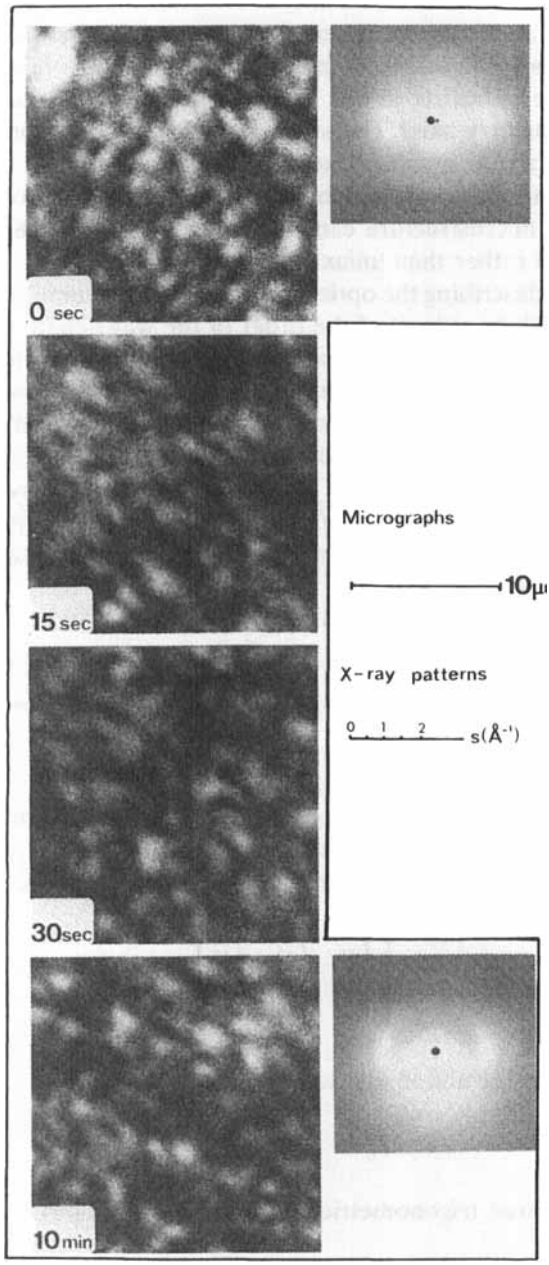

FIGURE 11 A sequence of micrographs of B-ET at 220°C. As with B-N (Figure 10), the texture is mobile, but the X-Ray orientation has decayed little over 10 minutes.

is distributed about the specimen symmetry axis at an angle β, then what are the possible orientations of the principal axes of the elliptical section of the indicatrix in the specimen plane and parallel to the specimen symmetry axis? The significance of the question is to determine whether the apparent lack of correlation between the X-Ray orientation and the local orientation of the optically anisotropic domains of the microstructure can be accounted for by the polymers having biaxial rather than uniaxial optical properties.

The tensor describing the optical properties of a volume of polymer, having dimensions at least of the order of the wavelength of light, is usefully represented as an optical indicatrix. The biaxial indicatrix is an ellipsoid with the three principal axes having lengths proportional to the three different principal refractive indices. Such an indicatrix is depicted in Figure 12 in an arbitrary orientation with respect to the three laboratory axes, X, Y and Z, to which it is related by the three Euler angles† α, β and γ. The Y-Z plane is the specimen plane, with Z being parallel to the macroscopic symmetry axis of the sample (the extrusion axis).

The tensor which the indicatrix represents can also be written as:

$$\begin{bmatrix} T_{11} & 0 & 0 \\ 0 & T_{22} & 0 \\ 0 & 0 & T_{33} \end{bmatrix}$$

Only components of the leading diagonal are present, since the tensor is referred to its principal axes (a, b and c in Figure 12). Transformed to the laboratory axes, X, Y, and Z, the tensor becomes:

$$\begin{bmatrix} T'_{11} & T'_{12} & T'_{13} \\ T'_{21} & T'_{22} & T'_{23} \\ T'_{31} & T'_{32} & T'_{33} \end{bmatrix}$$

where the transformation law is:

$$T'_{ij} = \Sigma_k a_{ik} a_{jk} T_{kk}$$

and a_{mn} is related trigonometrically to the Euler angles.

---

†Due to convention of use, the symbol α is required in two contexts in this paper. From this point onwards it will represent an Euler angle, and not a coordinate in the depiction of two-dimensional X-Ray intensity functions.

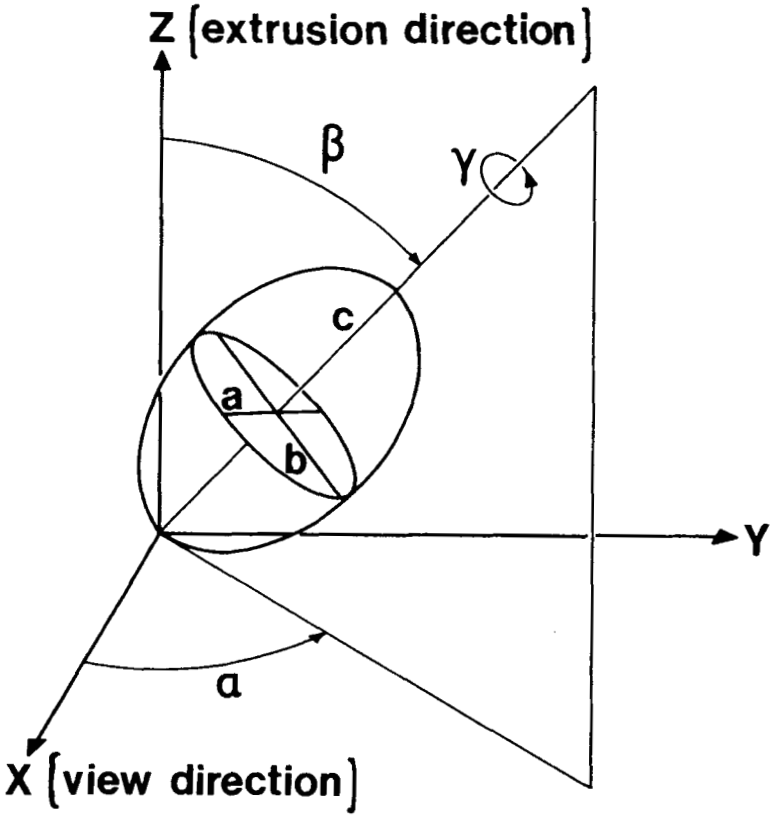

FIGURE 12 Diagram relating the orientation of the biaxial optical indicatrix, having principal axes a, b, and c, to the laboratory axes (X, Y, Z). The following conditions are taken to define $\gamma = 0°$: $\alpha = \beta = 0°$ and $a \parallel X$.

The extinction directions observed in the microscope are determined by the orientation of the principal axes of the elliptical central section of the indicatrix which is parallel to the specimen plane, YZ. The ellipse is described by the four terms in the bottom right-hand corner of the symmetric tensor above i.e.:

$$\begin{bmatrix} T'_{22} & T'_{23} \\ T'_{32} & T'_{33} \end{bmatrix}$$

By diagonalising this symmetric tensor, its principal axes can be found:

$$\begin{vmatrix} T'_{22} - \lambda & T'_{23} \\ T'_{32} & T'_{33} - \lambda \end{vmatrix} = 0$$

$$\therefore \lambda = \frac{T'_{22} + T'_{33}}{2} + \left[\left(\frac{T'_{22} + T'_{33}}{2} \right)^2 + (T'_{23})^2 \right]^{1/2} \quad (1)$$

The optically slow vibration direction is identified by the solution containing the positive square root (i.e. λ_+). Its orientation, measured as the angle θ relative to Y in the specimen plane, is given by (Appendix 2):

$$\cot\theta = \frac{\lambda_+ - T'_{23} - T'_{33}}{-\lambda_+ + T'_{23} + T'_{22}} \quad (2)$$

The value of θ for various values of α, β and γ, given the magnitudes of (a, b, c), can be readily computed.

It is apparent that, for a given optical indicatrix, the value of θ changes as α, β and γ change. Of particular relevance in this context is how θ changes if one is dealing with an assemblage of anisotropic units in which β is fixed but α and γ are permitted to vary. A variation in γ represents the rotation of the indicatrix about one of its principal axes, and if this axis is identified with the direction of the molecular director in the unit, then γ can be considered to vary without any consequent change in the director orientation such as might be determined by diffraction. It can be shown (Appendix 3) that **any** value of θ can be obtained by a suitable choice of γ, for **at least one** value of α, if the shape of the optical indicatrix lies within the limits:

$$\frac{2(1 - T' \sin^2\beta)}{(1 + T')\cos^2\beta} \leqslant L \leqslant \frac{2(T' - \sin^2\beta)}{(1 + T')\cos^2\beta}; \quad \beta < 45° \quad (3)$$

Where:

$$L = 2c/(a + b),$$

and

$$T = b/a \quad \text{while} \quad T' = T \text{ if } T > 1, \quad \text{and} \quad T' = 1/T \text{ if } T < 1.$$

It follows that for samples with macroscopic uniaxial symmetry, such as those under consideration, in which all values of α and γ can occur, the extinction directions within the specimen plane will have orientations within the full 2π angular range, provided that the above inequality holds. The ranges of values of L and T (describing the indicatrix shape) within which all values of θ are achievable with appropriate settings of α and γ are shown in Figure 13 for four fixed values of β. Note that for the case of a uniaxial indicatrix, with c as its unique axis ($a = b$ or $T = 1$), there are no values of L for which all values of θ can be achieved, except for the trivial case of $L = 1$ which corresponds to an optically isotropic material.

It is important to state that within the α -- γ domain all values of θ may not occur with equal frequency, although a complete explanation of the observed optical textures requires a reasonably uniform distribution after the appropriate integration has been performed over the distribution of angles β which is present in the sample. Figure 14 is a map of the orientations of the slow vibration direction (major axis of the ellipse in the specimen plane) within the $\alpha - \gamma$ domain. It is calculated for values of $\beta = 30°$, $T = 2.0$ and $L = 1.3$, and thus corresponds to an optical anisotropy rather more marked than is likely to be encountered even in such potentially strongly birefringent polymers as those examined. Nevertheless the orientations are reasonably evenly represented.

It has thus been demonstrated that, for an optically biaxial material in which one principal axis of the indicatrix is considered to be aligned with the local molecular director, as defined by the 'fibre axis' of the diffraction pattern from the same region, a preferred orientation of these directors in the sample as a whole need not necessarily lead to a preferred orientation of the optical extinction axes in the specimen plane.

For the sake of completeness it is necessary to consider if it is at all possible for the local anisotropic regions to have *uniaxial* properties, yet with there being no special relationships between the orientation of the unique axis and the preferred orientation of the molecular chain segments. For, if this is possible, another level of geometric complexity must be added to the above treatment where a principal axis of the indicatrix was set parallel to the local molecular director. Neumann's Principle[22] states that the symmetry elements of any physical property must include the symmetry elements of the point group of the region in question. Thus for all point groups except triclinic, symmetry considerations demand a special relationship. In the case of triclinic, the indicatrix will be general and thus biaxial. It is possible

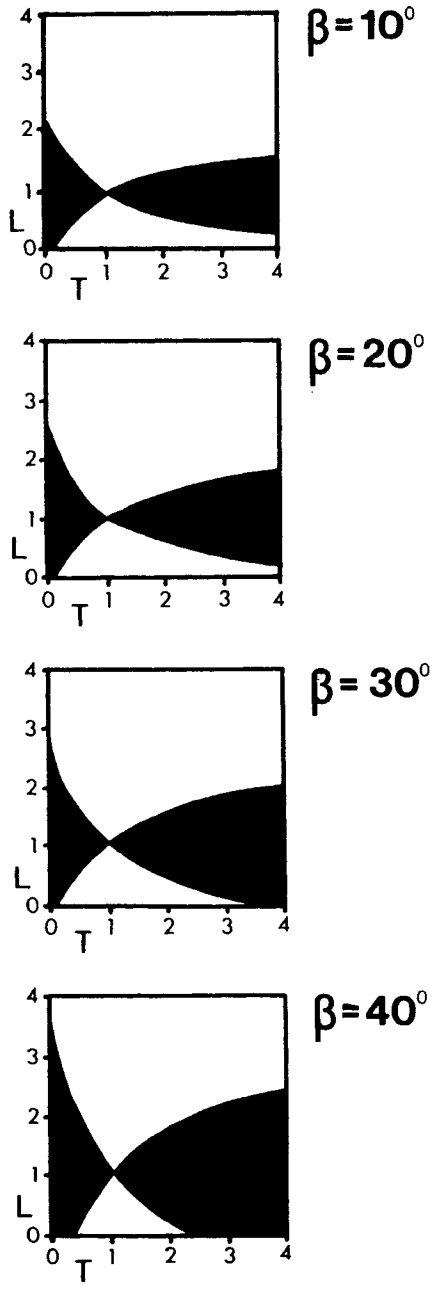

FIGURE 13 Ranges of the parameters T and L (describing the shape of the biaxial indicatrix) for which all orientations of the extinction direction in the specimen plane are possible given appropriate settings of α and γ, at the fixed values of β shown.

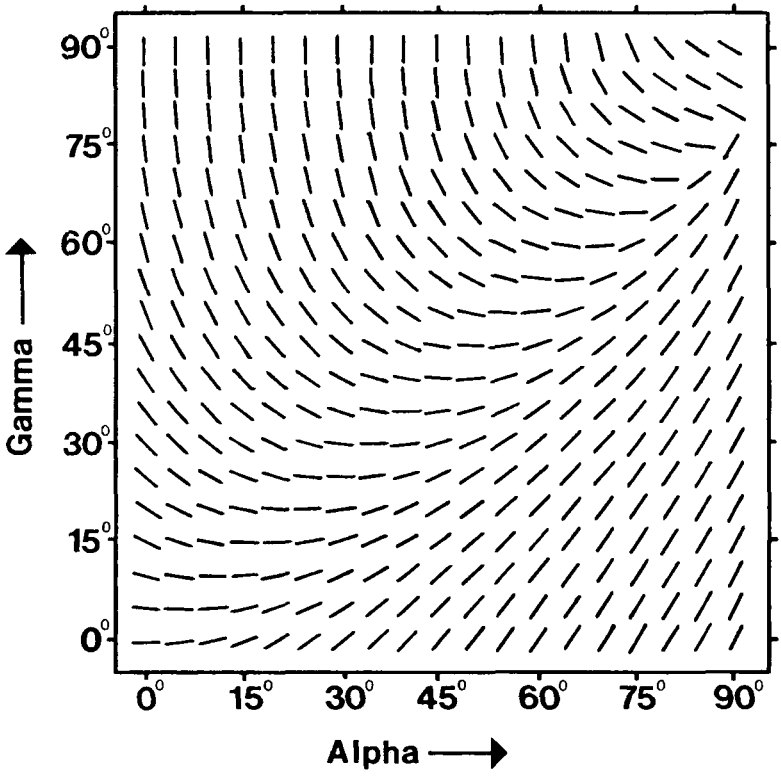

FIGURE 14 Map showing the orientations of the slow extinction direction, as a function of α and γ, for one particular example of an indicatrix (shape given by T = 2 and L = 1.3) and one fixed value of β (30°).

that, by chance, two of its principal refractive indices (or even all three) will be so similar as to be indistinguishable experimentally, but the occurrence of such a chance match in **both** the polymers under consideration is discounted. Additionally, triclinic structural symmetry implies rotational correlation of the molecules about all three axes in any case.

STRUCTURAL IMPLICATIONS OF OPTICAL BIAXIALITY

The only explanation of the disparity between the orientation apparent in the X-Ray diffraction patterns and the absence of preferred orientation of the axes describing the local optical anisotropy is to consider the polymers to be optically biaxial. Such a proposal has

been shown to be viable for certain ranges of indicatrix shape, where only one principal axis of the indicatrix (c) is defined in relation to the macroscopic sample axis (extrusion direction), being set at a fixed angle to it (β).

Optical biaxiality implies not only that the molecules themselves possess more than uniaxial symmetry, which is very possible for the copolyesters considered, but also that they are orientationally correlated with their neighbours about all three axes over distances of a μm or so. The sequence of aromatic groups along a polyester molecule, which because of conjugational energies will tend to be coplanar with the ester groups, provides the possibility of a lath-like molecule and hence orientation correlation about three axes. On the other hand, conformational energy calculations,[23] indicate a steric hinderance preventing coplanarity between an aromatic ring and a neighbouring ester where they are joined through the singly bonded oxygen atom. Alternatively it is possible that the full orientational correlation is achieved through the electrostatic dipole forces between neighbouring ester groups on adjacent chains.

In seeking the appropriate structural classification for these non-chiral polymers one is faced with the choice between nematic and smectic. The unsuitability of describing B-ET as a smectic has been discussed elsewhere.[14] Small angle X-Ray scattering curves for B-N (Figure 15) show no maxima which could be associated with the long range density wave normally held to be characteristic of the smectic phase; furthermore, although they were prepared from an oriented sample, they show no indication of the axial alignment so apparent in the equivalent wide angle X-Ray scans. However, in identifying the phase as nematic, it should also be noted that cylindrical distribution functions of B-ET[24] show evidence of **at least** short range longitudinal register between aromatic groups on neighbouring chains. Whether such register, if it were to extend over longer ranges without crystallization, would warrant smectic classification is an open question.

At this stage the weight of evidence is that above the softening temperature the mesophase is nematic and optically biaxial. Following Frank[25] the structural description 'biaxial nematic' is avoided, 'biaxial' describing an optical **property** represented by a particular class of an indicatrix, and the term 'multiaxial nematic' is used instead. Multiaxial nematics have been proposed on theoretical grounds a number of times for low molar mass liquid crystals,[26-29] although they are not normally seen, as the uniaxial-multiaxial transition temperature (on cooling) is likely to be below the crystallization temperature.

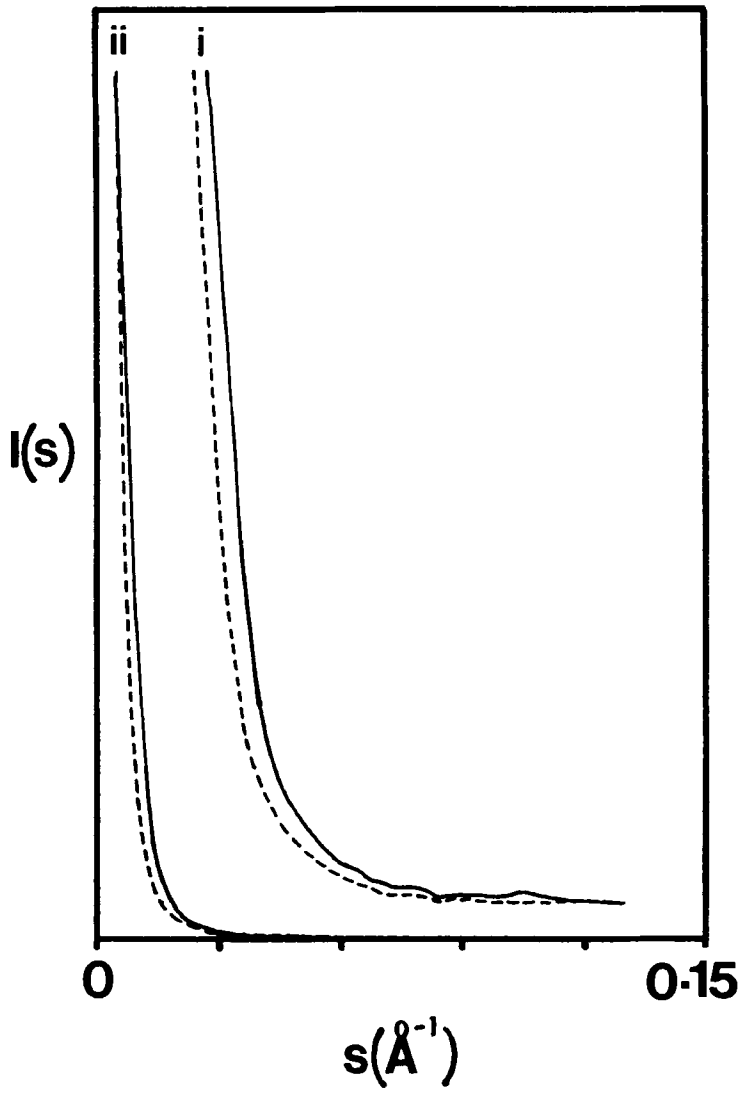

FIGURE 15 Small angle X-Ray diffraction scans of the polymer B-N. The curves (i) and (ii) are plotted from the same set of data, but the vertical scale of (i) has been magnified 100× relative to that of (ii). The scattering was measured from a section of oriented material containing the extrusion axis; the continuous lines represent a profile for scattering in the meridional plane (containing the incident beam and the extrusion axis) while the dashed lines are an equatorial profile.

However, in the polymers considered, where crystallization has been suppressed by the technique of copolymerization, the multiaxial nematic phase region is stable.

CONCLUSIONS

1. In the liquid state both polymers exhibit birefringent microstructures which are characteristic of liquid crystallinity. The scale of the Schlieren-type textures is much finer than that normally seen with low molar mass liquid crystals; however, they do not change on cooling to the solid phase at room temperature.

2. Specimens cooled from extruded melts give wide angle X-Ray diffraction patterns with pronounced axial orientation reflecting a preferred orientation of the local chain axes of the molecules. There is **no** corresponding preferred orientation in the microstructure of thin sections cut to include the extrusion axis, the axes describing the local optical anisotropy assuming different orientations with equal frequency across the complete section.

3. The facts of preferred orientation in the X-Ray diffraction patterns and the lack of it in the optical texture can be reconciled if the polymer is optically biaxial.

4. The absence of any long period density waves, and the presence of biaxial optical properties, indicates that the mesophase should be classified as a nematic with orientation correlations about all three axes. The structure is described as a **multiaxial nematic** in preference to the term 'biaxial nematic.'

Acknowledgments

The authors wish to thank Sir Charles Frank for discussion, Drs. B. Griffin of ICI, M. Jaffe of Celanese Corporation, and W. J. Jackson of Tennessee Eastman for the supply of samples, Dr. O. Yoda for making the small angle X-Ray measurements, and the SERC for funding.

Appendix 1

This appendix shows in outline how a superimposed sequence of discrete optically anisotropic layers is equivalent to a single optically anisotropic unit, with the orientation of the in-plane axes lying between those of the component layers.

Superposition of two linearly birefringent layers:

Figure A1.1 defines the necessary angles and directions. Light of unit amplitude transmitted by the polariser can be described formally by the expression: $\exp\{i\omega t\}$. This is resolved along the optical vibration directions of the first layer; on leaving the layer these components

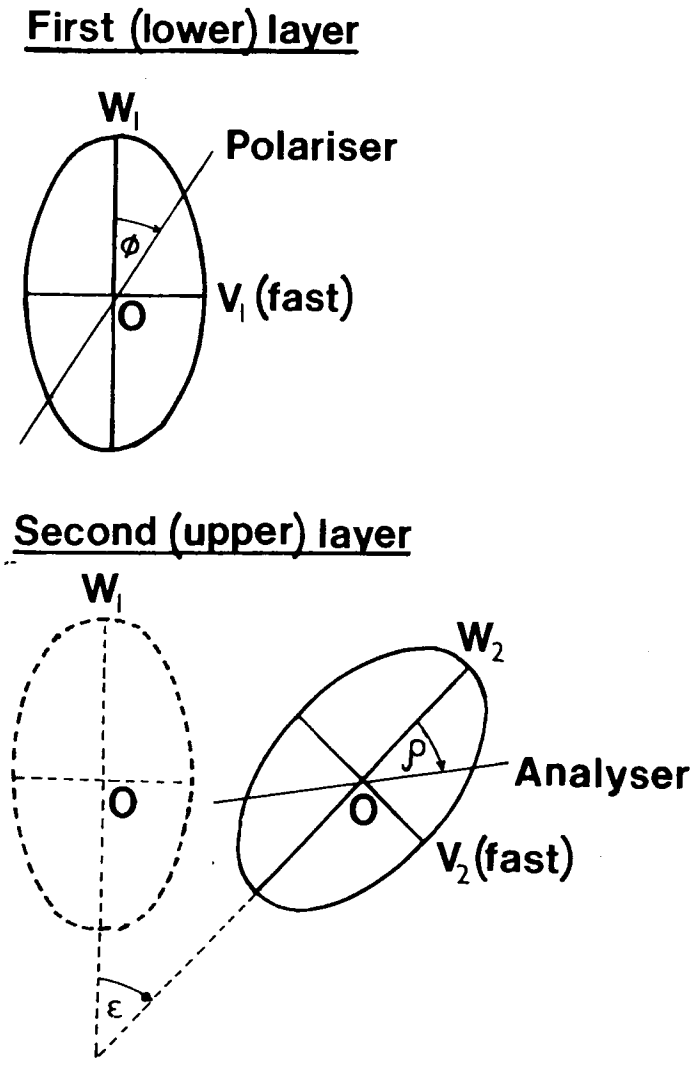

FIGURE A1.1 Geometry of two superimposed linearly birefringent units, viewed between polariser and analyser. The angles and directions defined here are referred to in Appendix 1.

are:

(along OW_1) $\exp\{i(\omega t - \delta_1)\}\cos\phi$

(along OV_1) $\exp\{i\omega t\}\sin\phi$, where δ_1 represents the phase difference which the layer introduces between light waves traveling along OW_1 and OV_1.

On entering the second layer, each of these components is resolved into two further components, along OW_2 and OV_2. These are subsequently resolved into the transmission direction of the analyser.

If the analyser and polariser are crossed, $(\rho + \epsilon) - \phi = 90°$, and the amplitude transmitted by the analyser is given by:

$$A_R = [\sin\epsilon\cos\rho + \cos\epsilon\sin\rho]\cos\epsilon\cos\rho\exp\{i(\omega t - \delta_1 - \delta_2)\}$$

$$- [\cos\epsilon\cos\rho - \sin\epsilon\sin\rho]\sin\epsilon\cos\rho\exp\{i(\omega t - \delta_2)\}$$

$$- [\sin\epsilon\cos\rho + \cos\epsilon\sin\rho]\sin\epsilon\sin\rho\exp\{i(\omega t - \delta_1)\}$$

$$- [\cos\epsilon\cos\rho - \sin\epsilon\sin\rho]\cos\epsilon\sin\rho\exp i\omega t$$

The *intensity* of the transmitted light is given by:

$$I = A_R \cdot A_R^*$$

Application of standard formulae for the sum, difference or product of trigonometric functions leads to the result:

$$I = \frac{1}{2}\sin^2 2\epsilon(1 - \cos\delta_1)$$

$$+ \frac{1}{2}\sin^2 2\rho[1 - \cos\delta_1\cos\delta_2 + \cos 2\epsilon\sin\delta_1\sin\delta_2$$

$$- \sin^2 2\epsilon(1 - \cos\delta_1 + \cos\delta_2 - \cos\delta_1\cos\delta_2)]$$

$$+ \frac{1}{8}\sin 4\rho\ [2\sin 2\epsilon\sin\delta_1\sin\delta_2$$

$$+ \sin 4\epsilon(1 - \cos\delta_1 + \cos\delta_2 - \cos\delta_1\cos\delta_2)]$$

This can be written in the form:

$I = A + B\sin^2 2\rho + C\sin 4\rho$, where A, B and C are independent of ρ. i.e. the transmitted intensity is in general never zero, the exception being the special case $\epsilon = 0, \pi/2, \pi, 3\pi/2, \ldots$ For a maximum/minimum in transmitted intensity as the crossed polars are rotated relative to the specimen:

$$\frac{dI}{d\rho} = 0.$$

This gives:

$$\tan 4\rho = -\frac{2C}{B} \qquad \text{(A1.1)}$$

This equation has 8 solutions in the range $0 \leq \rho < 2\pi$, corresponding to 4 intensity maxima and 4 intensity minima during a 2π rotation of the crossed polars. Implied in this result is the fact that, if two layers consisting of an array of similarly-sized optically anisotropic domains are superimposed, the texture observed between crossed polars should have the same scale as that seen with a single layer. Only the range of *contrast* is changed relative to the single layer case.

It is now also possible to address the question as to whether an arbitrary orientation of the "axes of minimum intensity," relative to an external axis, can be obtained by superimposing two optically anisotropic layers having appropriate birefringences, given a particular relative orientation of their slow vibration directions. To find the answer it is necessary to investigate how those values of ρ which define the axes of minimum intensity (as calculated from A1.1) change when the *difference* in birefringence of the two layers is varied and the given relative orientation of the two layers is maintained. In order to vary the difference in birefringence, it is only necessary to vary the birefringence of one layer (δ_1, say) while keeping that of the other layer (δ_2) a constant. Equation A1.1 can be rewritten as:

$$\rho = -\frac{1}{4}\tan^{-1}\frac{f(\delta_1)}{g(\delta_1)}, \qquad \begin{array}{l}\text{if } \delta_1 \text{ is vairable while } \delta_2 \\ \text{and } \epsilon \text{ are held constant.}\end{array}$$

The extreme values for ρ for an axis of minimum intensity are now given by:

$$\frac{\partial \rho}{\partial \delta_1} = 0$$

This in turn requires that:

$$\frac{\partial f}{\partial \delta_1} g - f \frac{\partial g}{\partial \delta_1} = 0$$

An axis of minimum intensity is always found to lie within the range $\rho = 0$ to $\rho = -\epsilon$, i.e. the orientation of the axes of minimum intensity is constrained to the extent that one of them always lies within the acute angle bounded by the slow vibration directions of the two layers, whatever the relative birefringences of those layers.

Superposition of more than two linearly birefringent layers

This case can be covered by a qualitative extension of the above argument. If, for example, one is dealing with three layers, the bottom and middle ones can be regarded as a single unit, having one axis of minimum intensity oriented within limits as described above. The effect of then superimposing the top layer is to shift the orientation of this axis towards the slow vibration direction of the top layer. The net result is that the orientation of one axis of minimum intensity of the three-layer specimen lies somewhere within the range of orientations described by the slow vibration directions of the superimposed layers.

It is also apparent that, if a specimen shows extinction between crossed polars, it cannot consist of a succession of superimposed discrete layers, except in the special case where the layers are stacked with their vibration directions parallel.

Appendix 2

This appendix shows how the orientation of the slow vibration direction in the YZ plane can be calculated for any given orientation of the (biaxial) optical indicatrix.

The slow vibration direction in the YZ plane is a principal axis of that elliptical central indicatrix section which is parallel to the YZ plane. Therefore, by the definition[22] of a principal axis A:

$T'_{ij}A_j = \lambda_+ A_i$, where λ_+ is a constant, given by equation 1.

$$\therefore\ T'_{22}A_2 + T'_{23}A_3 = \lambda_+ A_2 \text{ and } T'_{32}A_2 + T'_{33}A_3 = \lambda_+ A_3$$

$$\therefore\ T'_{22}|A|l_2 + T'_{23}|A|l_3 = \lambda_+ |A|l_2, \text{ and}$$

$$T'_{32}|A|l_2 + T'_{33}|A|l_3 = \lambda_+ |A|l_3,$$

where l_2 and l_3 are direction cosines relating the slow vibration direction to Y and Z respectively.

$$\therefore T'_{22}l_2 + T'_{23}l_3 = \lambda_+ l_2 \quad \text{and} \quad T'_{32}l_2 + T'_{33}l_3 = \lambda_+ l_3.$$

These equations can be combined to give:

$$\frac{l_2}{l_3} = \frac{\lambda_+ - T'_{23} - T'_{33}}{-\lambda_+ + T'_{23} + T'_{22}}$$

($T'_{23} = T'_{32}$ because these are components of a symmetric tensor.) If θ is defined as the angle between the slow vibration direction and Y, $l_2 = \cos\theta$ and $l_3 = \sin\theta$.

$$\therefore \cot\theta = \frac{\lambda_+ - T'_{23} - T'_{33}}{-\lambda_+ + T'_{23} + T'_{22}}$$

Appendix 3

This appendix shows how limits can be found for the shape of optical indicatrix, within which any value of θ can be obtained by a suitable choice of γ, for at least one value of α.

The equations 1 and 2 can be combined to give:

$$(U - V)\cot\theta = U + V, \text{ where } U = \frac{T'_{22} - T'_{33}}{2}$$

$$\text{and } V = [U^2 + (T'_{23})^2]^{1/2} - T'_{23}$$

For this to be satisfied by any value of θ:

$$\begin{aligned} U + V &= U - V = 0 \\ \therefore\ T'_{22} &= T'_{33} \end{aligned} \qquad \text{(A2.1)}$$

This condition can be related back to the principal axes T_{kk} of the optical indicatrix via the transformation law for second rank tensors

$$T'_{ij} = \Sigma_k a_{ik} a_{jk} T_{kk}.$$

The a_{mn} are in turn related trigonometrically to the Euler angles (α, β, γ).[30]

If additionally the substitutions $T = \frac{T_{22}}{T_{11}}$ and $L = \frac{2T_{33}}{T_{11} + T_{22}}$ are made, the condition A2.1 then becomes:

$$L = 2\left\{\frac{(s\beta c\gamma)^2 - (c\alpha s\gamma + s\alpha c\beta c\gamma)^2 + (s\beta s\gamma)^2 T - (c\alpha c\gamma - s\alpha c\beta s\gamma)^2 T}{(1 + T)(s^2\alpha s^2\beta - c^2\beta)}\right\} \tag{A2.2}$$

(The abbreviations s = sin and c = cos have been used, to allow A2.2 to be written in a compact form.)

Since the quantities sinα, cosα, sinβ, cosβ, sinγ, cosγ and T are all continuous, the result of adding, subtracting, multiplying or dividing them is also continuous, provided that division by 0 does not occur anywhere.[31]

So L is continuous if the denominator of A2.2 is not equal to 0, which is assured if $\beta < 45°$. This is in keeping with the application of this model to a system of molecules having a high degree of preferred chain segment alignment.

The value of establishing the continuity of L lies in that, if one can identify an absolute maximum and an absolute minimum for L, in terms of the independent variables contained in A2.2, one can be sure that intermediate values of L correspond to real values of these variables.

Our model seeks to relate changes in θ to variations in γ, representing a rotation of the indicatrix about the principal axis which coincides with the local molecular director. So the stationary points in L must be found by solving:

$$\frac{\partial L}{\partial \gamma} = 0, \text{ with } \alpha, \beta \text{ and } T \text{ held constant.}$$

This gives:

$$T = 1 \text{ (for all } \alpha, \beta, \gamma) \tag{A2.3}$$

$$\text{or } \gamma = 0° \text{ or } 90°, \text{ together with } \alpha = 0° \text{ or } 90° \text{ (for all } T, \beta) \tag{A2.4}$$

$$\text{or } \tan 2\gamma = \frac{\sin 2\alpha \cos\beta}{\sin^2\alpha\cos^2\beta - \cos^2\alpha - \sin^2\beta} \text{ (for all } T) \tag{A2.5}$$

The case of A2.3 is a trivial one, corresponding to the indicatrix being uniaxial.

The case A2.4 needs more careful examination: The conditions $\alpha = 0°$ and $\alpha = 90°$ are in turn substituted into equation A2.2, and the sign of $\frac{\partial^2 L}{\partial \gamma^2}$ is found in each case for both $\gamma = 0°$ and $\gamma = 90°$. The following results are obtained:

$$\frac{\partial^2 L}{\partial \gamma^2} < 0 \text{ (i.e. } L \text{ has a maximum)} \quad \begin{aligned} &\text{if } \alpha = 0°, \gamma = 0° \text{ and } T > 1 \\ &\text{or } \alpha = 0°, \gamma = 90° \text{ and } T < 1 \\ &\text{or } \alpha = 90°, \gamma = 0° \text{ and } T < 1 \\ &\text{or } \alpha = 90°, \gamma = 90° \text{ and } T > 1 \end{aligned}$$

and

$$\frac{\partial^2 L}{\partial \gamma^2} > 0 \text{ (i.e. } L \text{ has a minimum)} \quad \begin{aligned} &\text{if } \alpha = 0°, \gamma = 0° \text{ and } T < 1 \\ &\text{or } \alpha = 0°, \gamma = 90° \text{ and } T > 1 \\ &\text{or } \alpha = 90°, \gamma = 0° \text{ and } T > 1 \\ &\text{or } \alpha = 90°, \gamma = 90° \text{ and } T < 1 \end{aligned}$$

It is possible to establish which of these are absolute extrema and which are relative extrema, by re-substituting each of the above sets of conditions into equation A2.2, and comparing the magnitudes of the values of L thus obtained. It is found that:

$$\frac{2(1 - T' \sin^2\beta)}{(1 + T')\cos^2\beta} \leqslant L \leqslant \frac{2(T' - \sin^2\beta)}{(1 + T')\cos^2\beta}, \qquad \text{(A2.6)}$$

if $T' = T$ when $T > 1$ and $T' = 1/T$ when $T < 1$.

Provided that L lies within these limits, a suitable choice of γ will enable any desired value of θ to be obtained, for at least one value of α.

A computer check can be used to demonstrate the correctness of these limits. From this it also follows that the stationary points defined for L by A2.5 can represent no more than relative extrema.

References

1. V. P. Shibaev and N. A. Plate, *Polymer Sci. USSR*, **19**, 1065 (1977).
2. J. H. Wendorff, H. Finkelmann and H. Ringsdorf, *J. Polym. Sci., Polym. Symp.*, **63**, 245 (1978).

3. E. T. Samulski and D. B. DuPré, *Advances in Liquid Crystals*, **4**, 121 (1979).
4. H. Finkelmann, in *Liquid Crystals in One or Two Dimensions*, ed. W. Helfrich and G. Heppke (Springer-Verlag, Berlin, 1980), pp. 238.
5. A. Blumstein, K. N. Sivaramakrishnan, R. B. Blumstein and S. B. Clough, *Polymer*, **23**, 47 (1982).
6. A. Blumstein and S. Vilasagar, *Mol. Cryst. Liq. Cryst. Letts.*, **72**, 1 (1981).
7. H. Finkelmann, *Phil. Trans. R. Soc. Lond.*, **A309**, 105 (1983).
8. M. G. Friedel, *Ann. de Physique*, **18**, 273 (1922).
9. D. Demus and L. Richter, *Textures of Liquid Crystals* (Verlag Chemie, Berlin, 1978).
10. G. W. Calundann, *U.S. Pat.*, 41 61 470 (1979).
11. R. A. Chivers, J. Blackwell and G. A. Gutierrez, *Polymer*, **25**, 435 (1984).
12. G. R. Mitchell and A. H. Windle, *Coll. and Polym. Sci.*, In press.
13. W. J. Jackson and H. F. Kuhfuss, *J. Polym. Sci., Polym. Chem.*, **14**, 2043 (1976).
14. C. Viney and A. H. Windle, *J. Mat. Sci.*, **17**, 2661 (1982).
15. M. R. Mackley, F. Pinaud and G. Siekmann, *Polymer*, **22**, 437 (1981).
16. G. R. Mitchell and A. H. Windle, *Polymer*, **24**, 1513 (1983).
17. G. R. Mitchell, unpublished work.
18. C. Viney, G. R. Mitchell and A. H. Windle, *Polymer Comm.*, **24**, 145 (1983).
19. C. Viney, *Laboratory Practice*, **32**, 87 (1983).
20. C. Viney, PhD Thesis, Cambridge University (1983).
21. C. Viney, A. M. Donald and A. H. Windle, *Polymer*, In press.
22. J. F. Nye, *Physical Properties of Crystals* (Clarendon Press, Oxford, 1957).
23. J. P. Hummel and P. J. Flory, *Macromolecules*, **13**, 479 (1980).
24. G. R. Mitchell and A. H. Windle, *Polymer*, **23**, 1269 (1982).
25. F. C. Frank, *Phil. Trans. R. Soc. Lond.*, **A309**, 71 (1983).
26. M. J. Freiser, *Phys. Rev. Lett.*, **24**, 1041 (1970).
27. C. S. Shih and R. Alben, *J. Chem. Phys.*, **57**, 3055 (1972).
28. J. P. Straley, *Phys. Rev.*, **A10**, 1881 (1974).
29. G. R. Luckhurst and S. Romano, *Mol. Phys.*, **40**, 129 (1980).
30. G. B. Arfken, *Mathematical Methods for Physicists* (Academic Press, New York, 1970) pp. 179.
31. M. R. Spiegel, *Advanced Calculus* (McGraw-Hill, New York, 1974) pp. 25.